$K \to e\nu$ decays and lepton flavor violation searches with Kaons

T. Spadaro
Laboratori Nazionali di Frascati dell'INFN, Frascati, Italy

Recent Kaon decay studies seeking for lepton-flavor violating (LFV) new-physics effects are briefly discussed. The main focus is set on precise measurements of rare or not-so-rare decays aiming at finding evidence of deviations from the SM prediction rather than on the results from direct searches of LFV transitions forbidden or ultra-rare in the SM.

I. INTRODUCTION

A significant effort has been devoted along the years to isolate signals from lepton flavor violating (LFV) transitions, which are forbidden or ultra-rare in the Standard Model (SM). The sensitivity to decays such as $\mu \to e\gamma$, $\mu \to eee$, $K_L \to \mu e(+\pi^0\text{'s})$, and others roughly improved by two orders of magnitude for each decade [1]. The activity in this field is still alive, with results coming until recently [2]. No signal has been observed, thus ruling out SM extensions with LFV amplitudes with mediator masses below ~ 100 TeV.

These results allowed the focus to be put on the detection of NP-LFV effects in loop amplitudes, by studying specific processes suppressed in the SM. Kaon physics is very well suited to match the precisions required for this task, the experiments benefiting from low background level and the theoretical predictions carefully accounting for radiative corrections to reach uncertainties of the level of 0.1% or better.

In the SM, electrons and muons differ only by mass and coupling to the Higgs. This allows the seeking of deviations from prediction in semileptonic (K_{l3}) and leptonic (K_{l2}) kaon decays.

Precise measurements of the semileptonic decay widths have been performed in recent years to extract the V_{us} parameter of the CKM matrix. The following expression is used:

$$\Gamma^i(K_{e3(\gamma),\,\mu 3(\gamma)}) \;=\; |V_{us}|^2 \frac{C_i^2 G^2 M^5}{128\pi^3} S_{\rm EW} \; |f_+^{K^0}(0)|^2 I^i_{e3,\,\mu 3}\,(1+\delta^i_{e3,\,\mu 3}),$$

where i indexes $K^0 \to \pi^-$ and $K^+ \to \pi^0$ transitions for which $C_i^2 = 1$ and $1/2$, respectively, G is the Fermi constant, M is the appropriate kaon mass, and $S_{\rm EW}$ is a universal short-distance electroweak correction [3]. The δ^i term accounts for long-distance radiative corrections depending on the meson charges and lepton masses and, for $K^\pm$, for isospin-breaking effects. These corrections are presently known at the few-per-mil level [4]. The $f_+^{K^0}(0)$ form factor parametrizes the vector-current transition $K^0 \to \pi^-$ at zero momentum transfer t, while the dependence of vector and scalar form factors on t enter into the determination of the integrals $I_{e3,\,\mu 3}$ of the Dalitz-plot density over the physical region. Four experiments with different techniques provided a new comprehensive set of measurements for all of the quantities appearing in the above equation. Results have been obtained for K_L (KLOE [5–7], KTeV [8], NA48 [9, 10]), $K^\pm$ (KLOE [11, 12], NA48 [13]), K^- (ISTRA+ [14]), and K_S (KLOE [15, 16]). The results for $|f_+^{K^0}(0)V_{us}|$ are averaged taking the error correlations into account [17]. The measurements are compatible among each other, with an average of $|f_+^{K^0}(0)V_{us}| = 0.2166(5)$ and a fit χ^2 probability of 58%.

The universality of weak vector transitions dictates the equality of the effective coupling constants extracted for K_{e3} and $K_{\mu 3}$ decays. The ratio $R_{\mu e3}$ defined as

$$R_{\mu e} = \frac{\Gamma^i(K_{\mu 3(\gamma)}) I^i_{e3}(1+\delta^i_{e3})}{\Gamma^i(K_{e3(\gamma)}) I^i_{\mu 3}(1+\delta^i_{\mu 3})}, \qquad (1)$$

is indeed proved to be compatible with unity: $R_{\mu e} = 1.0043(52)$ [17]. This was not the case at the time of the 2004 PDG compilation [18]:

Mode	$R_{\mu e}$	
	FlaviaNet average 2007	PDG 2004
K_L	1.0049(61)	1.054(15)
$K^\pm$	1.0029(86)	1.019(13)

(2)

These results can be compared with those from the study of $\tau \to l\nu\nu$ decays, which are sensitive as well to LFV effects in weak vector decays. The world-average result from τ decays, $R_{\mu e} = 0.9998(40)$ [19], has comparable error with that from K decays.

Measurements of K_{l2} widths can be linked to new physics effects. The ratio of $K_{\mu 2}$ to $\pi_{\mu 2}$ decay widths might accept NP contributions from charged Higgs exchange [20, 21] in supersymmetric extensions of the SM with two Higgs doublets. The effect would be seen as a difference of the V_{us}/V_{ud} ratio extracted from $K_{\mu 2}$, $\pi_{\mu 2}$ and that extracted from K_{l3} and superallowed Fermi transitions ("0^+"):

$$\left|\frac{V_{us}(K_{l2})V_{ud}(0^+)}{V_{us}(K_{l3})V_{ud}(\pi_{l2})}\right| = \left|1 - \frac{m_K^2(m_s-m_d)\tan^2\beta}{M_H^2 m_s(1+\epsilon_0\tan\beta)}\right|,$$

where $\tan\beta$ is the ratio of up- and down-Higgs vacuum expectation values, M_H is the charged Higgs mass, and $\epsilon_0 \sim 0.01$ [22]. The world average result of this

ratio can be translated into a 95%-CL exclusion plot in the plane $\tan\beta$ vs M_H (see Fig. 1), showing that this analysis is complementary to and competitive with that [21] using the average $\mathrm{BR}(B \to \tau\nu) = 1.42(44) \times 10^{-4}$ of Babar and Belle measurements [23].

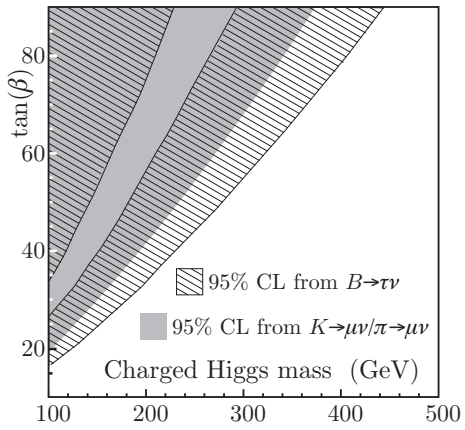

FIG. 1: Excluded regions at 95% CL from analysis of decays $K \to \mu\nu$ (filled area) and $B \to \tau\nu$ (hatched area).

A strong interest for a new measurement of the ratio $R_K = \Gamma(K^\pm \to e^\pm\bar{\nu_e})/\Gamma(K^\pm \to \mu^\pm\bar{\nu_\mu})$ has recently arisen, triggered by the work of Ref. [24].

The SM prediction of R_K benefits from cancellation of hadronic uncertainties to a large extent and therefore can be calculated with high precision. Including radiative corrections, the total uncertainty is less than 0.5 per mil [25]. Since the electronic channel is helicity-suppressed by the $V-A$ structure of the charged weak current, R_K can receive contributions from physics beyond the SM, for example from multi-Higgs effects inducing an effective pseudoscalar interaction. It has been shown in Ref. [24] that deviations from the SM of up to few percent on R_K are quite possible in minimal supersymmetric extensions of the SM and in particular should be dominated by lepton-flavor violating contributions with tauonic neutrinos emitted in the electron channel.

In order to compare with the SM prediction at this level of accuracy, one has to treat carefully the effect of radiative corrections, which contribute to nearly half the K_{e2} width. In particular, the SM prediction of Ref. [25] is made considering all photons emitted by the process of internal bremsstrahlung (IB) while ignoring any contribution from structure-dependent direct emission (DE). Of course both processes contribute, so in the analysis DE is considered as a background which can be distinguished from the IB width by means of a different photon energy spectrum.

Two experiments are participating in the challenge to push the error on R_K from the present 6% down to less than 1%. Last year, KLOE and NA48/2 announced preliminary results [26, 27] with errors ranging from 2% to 3%. Moreover, the new NA62 collaboration collected more than 100 000 K_{e2} events in a dedicated run of the NA48 detector, aiming at reaching an accuracy of few per mil on R_K. The analyses of $K_{e2}/K_{\mu2}$ in the KLOE and NAxx setups will be the main topic discussed here.

II. MEASURING R_K AT KLOE

DAΦNE, the Frascati ϕ factory, is an e^+e^- collider working at $\sqrt{s} \sim m_\phi \sim 1.02$ GeV. ϕ mesons are produced, essentially at rest, with a visible cross section of ~ 3.1 μb and decay into K^+K^- pairs with a BR of $\sim 49\%$.

Kaons get a momentum of ~ 100 MeV/c which translates into a low speed, $\beta_K \sim 0.2$. K^+ and K^- decay with a mean length of $\lambda_\pm \sim 90$ cm and can be distinguished from their decays in flight to one of the two-body final states $\mu\nu$ or $\pi\pi^0$.

The kaon pairs from ϕ decay are produced in a pure $J^{PC} = 1^{--}$ quantum state, so that observation of a K^+ in an event signals, or tags, the presence of a K^- and vice versa; highly pure and nearly monochromatic $K^\pm$ beams can thus be obtained and exploited to achieve high precision in the measurement of absolute BR's.

The analysis of kaon decays is performed with the KLOE detector, consisting essentially of a drift chamber, DCH, surrounded by an electromagnetic calorimeter, EMC. A superconducting coil provides a 0.52 T magnetic field. The DCH [28] is a cylinder of 4 m in diameter and 3.3 m in length, which constitutes a fiducial volume for $K^\pm$ decays extending for $\sim 1\lambda_\pm$, respectively. The momentum resolution for tracks at large polar angle is $\sigma_p/p \leq 0.4\%$. The c.m. momenta reconstructed from identification of 1-prong $K^\pm \to \mu\nu, \pi\pi^0$ decay vertices in the DC peak around the expected values with a resolution of 1–1.5 MeV, thus allowing clean and efficient $K^\mp$ tagging.

The EMC is a lead/scintillating-fiber sampling calorimeter [29] consisting of a barrel and two endcaps, with good energy resolution, $\sigma_E/E \sim 5.7\%/\sqrt{\mathrm{E(GeV)}}$, and excellent time resolution, $\sigma_T = 54\ \mathrm{ps}/\sqrt{\mathrm{E(GeV)}} \oplus 50$ ps. The timing capabilities of the EMC are exploited to precisely reconstruct the position of decay vertices of $K^\pm$ to π^0's from the cluster times of the emitted photons, thus allowing a precise measurement of the $K^\pm$ lifetime [11].

In early 2006, the KLOE experiment completed data taking, having collected ~ 2.5 fb^{-1} of integrated luminosity at the ϕ peak, corresponding to $\sim$3.6 billion K^+K^- pairs. Using the present KLOE dataset, the KLOE collaboration claims that an accuracy of about 1 % in the measurement of R_K might be reached.

Given the $K^\pm$ decay length of $\sim$90 cm, the selection of one-prong $K^\pm$ decays in the DC required to

tag $K^{\mp}$ has an efficiency smaller than 50%. In order to keep the statistical uncertainty on the number of $K^{\pm} \to e^{\pm}\bar{\nu_e}$ counts below 1%, a "direct search" for $K^{\pm} \to e^{\pm}\bar{\nu_e}$ and $K^{\pm} \to \mu^{\pm}\bar{\nu_\mu}$ decays is performed, without tagging. Since the wanted observable is a ratio of BR's for two channels with similar topology and kinematics, one expects to benefit from some cancellation of the uncertainties on tracking, vertexing, and kinematic identification efficiencies. Small deviations in the efficiency due to the different masses of e's and μ's will be evaluated using MC.

Selection starts by requiring a kaon track decaying in a DC fiducial volume (FV) with laboratory momentum between 70 and 130 MeV, and a secondary track of relatively high momentum (above 180 MeV). The FV is defined as a cylinder parallel to the beam axis with length of 80 cm, and inner and outer radii of 40 and 150 cm, respectively. Quality cuts are applied to ensure good track fits.

A powerful kinematic variable used to distinguish $K^{\pm} \to e^{\pm}\bar{\nu_e}$ and $K^{\pm} \to \mu^{\pm}\bar{\nu_\mu}$ decays from the background is calculated from the momenta of the kaon and the secondary particle measured in DC: assuming zero neutrino mass one can obtain the squared mass of the secondary particle, or lepton mass ($M^2_{\rm lep}$). The distribution of $M^2_{\rm lep}$ is shown in Fig. 2 for MC events before and after quality cuts are applied. While this selection is enough for clean identification of a $K^{\pm} \to \mu^{\pm}\bar{\nu_\mu}$ sample, further rejection is needed in order to identify $K^{\pm} \to e^{\pm}\bar{\nu_e}$ events: the background, which is dominated by badly reconstructed $K^{\pm} \to \mu^{\pm}\bar{\nu_\mu}$ events, is reduced by a factor of $\sim$10 by the quality cuts, but still remains $\sim$10 times more frequent than the signal in the region around the electron mass peak.

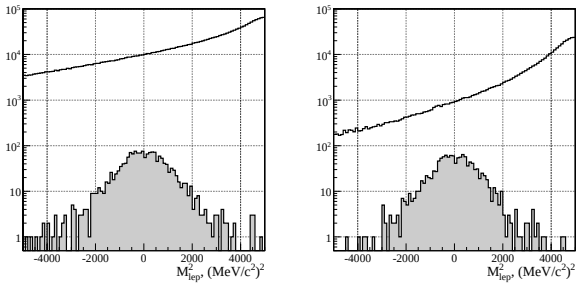

FIG. 2: MC distribution of $M^2_{\rm lep}$ before (left) and after (right) quality cuts are applied. Shaded histogram: $K^{\pm} \to e^{\pm}\bar{\nu_e}$ events. Open histograms: background, dominated by $K^{\pm} \to \mu^{\pm}\bar{\nu_\mu}$ events. In MC, R_K is set to the SM value.

Information from the EMC is used to improve background rejection. The secondary track is extrapolated to a position $\vec{r}_{\rm ext}$ on the EMC surface with momentum $\vec{p}_{\rm ext}$ and associated to the nearest calorimeter cluster satisfying the impact-parameter cut $d_\perp < 30$ cm, where $d_\perp = |\vec{p}_{\rm ext}/|p_{\rm ext}| \times (\vec{r}_{\rm ext} - \vec{r}_{\rm cl})|$. For electrons, the associated cluster is close to the EMC surface so that its position projected along the track $d_\parallel = |\vec{p}_{\rm ext} \cdot (\vec{r}_{\rm ext} - \vec{r}_{\rm cl})|$ is only a few cm. Moreover, for electrons the cluster energy $E_{\rm cl}$ is a measurement of the particle momentum $p_{\rm ext}$. Therefore the following condition is required in the plane $E_{\rm cl}/p_{\rm ext}$ vs $d_\parallel$ (see Fig. 3):

$$\left(\frac{d_\parallel[\text{cm}] - 2.6}{2.6}\right)^2 + \left(\frac{E_{\rm cl}/p_{\rm ext} - 0.94}{0.2}\right)^2 < 2.5. \quad (3)$$

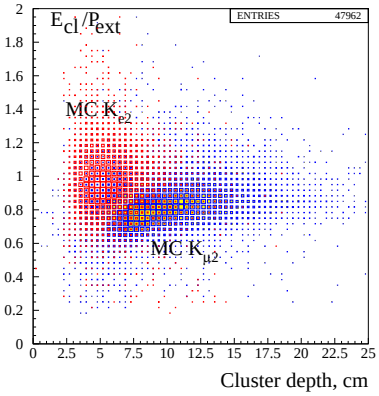

FIG. 3: MC distribution of the ratio $E_{\rm cl}/P_{\rm ext}$ of cluster energy and track momentum as a function of the depth of the cluster along the direction of impact of the secondary particle on the EMC.

Electron clusters can be further distinguished from μ (or π) clusters by exploiting the granularity of the EMC: electrons shower deposits their energy mainly in the first plane of EMC, while muons behave like minimum ionizing particles in the first plane and they deposit a sizable fraction of their kinetic energy from the third plane onward when they are slowed down to rest (Bragg peak).

The particle identification (PID) was therefore based on the asymmetry A_f of energy deposits between the second and the first planes hit, on the spread $E_{\rm RMS}$ of energy deposits on each plane, on the position $r_{\rm max}$ of the plane with the maximum energy, and on the asymmetry A_l of energy deposits between the last and the next-to-last planes. Muon clusters with the signature $A_f > 0$, or $x_{\rm max} > 12$ cm, or $A_l < -0.85$ are rejected. This criteria were optimized during MC and control sample studies.

The PID technique described above selects $K^{\pm} \to e^{\pm}\bar{\nu_e}$ events with an efficiency $\epsilon^{\rm PID}_{Ke2} \sim 64.7(6)\%$ and a rejection power for background of $\sim$ 300. These numbers have been evaluated from MC.

A likelihood fit to the two-dimensional $E_{\rm RMS}$ vs $M^2_{\rm lep}$ distribution was performed to get the number of signal events. Distribution shapes for signal and

background were taken from MC; the normalizations for the two components are the only fit parameters. The number of signal events obtained from the fit is $N_{Ke2} = 8090 \pm 156$. Projections of the fit results onto the two axes are compared to real data in Fig. 4.

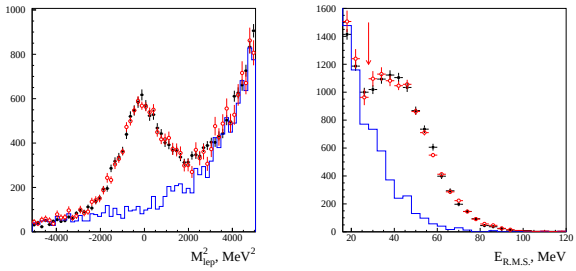

FIG. 4: Distributions of the lepton mass squared $E^2_{\rm lep}$ of the secondary track (left panel) and of the spread $E_{\rm RMS}$ of the energy deposits among the planes of the connected cluster in the EMC (right panel). Filled dots represent the data, open dots are the result of a maximum-likelihood fit using signal and background (solid line) distributions as input.

III. MEASURING R_K AT NA48 AND NA62

Unseparated, simultaneous, and highly collimated K^+ and K^- beams were designed to precisely measure the asymmetry in the dalitz-plot density for the decays $K^\pm \to \pi^\pm\pi^{+,0}\pi^{-,0}$ with the NA48/2 experiment.

The beams were produced by primary, 400-GeV protons from the SPS beam interacting with a beryllium target. After passing a selection system made of four dipole magnets with zero total deflection ("achromat") and various collimators, kaons enter a 114-m long, *sim*2-m in diameter, cylindrical fiducial decay volume $\sim$ 180 m after they are produced from the target, with a momentum of $\sim$ 60 GeV and a momentum bite of $\sim$ 3.8%. The NA48 detector is described in Ref. [30]. Kaon decay products are tracked by a magnetic spectrometer consisting of two pairs of drift chambers (DCHS) interleaved with a dipole magnet. The dipole provides a transverse momentum kick of $\sim$ 121 MeV. The relative momentum resolution from the tracking system is $\sigma_p/p \sim 1.02\% \oplus 0.044\%/p[\text{GeV}]$.

Particles emerging from the last drift chamber reach a hodoscope system made of scintillator slabs running along orthogonal views. This system is used for initiating the trigger and establishing the event time: the time resolution is $\sim$ 150 ps.

An e.m. calorimeter made of a LKr-filled volume closes the decay volume $\sim$ 240 m after the target. The calorimeter is read out by a fine-granularity system of accordion-shaped cathode rods providing highly uniform and efficient vetoing for photons impacting its 80×80 cm^2 surface, and guaranteeing excellent energy and transverse position resolutions for e.m. showers:

$$\sigma_E/E = 3.2\%/\sqrt{E[\text{GeV}]} \oplus 9\%/E[\text{GeV}] \oplus 0.42\% \quad (4)$$

$$\sigma_{x,y} = 4.2\text{mm}/\sqrt{E[\text{GeV}]} \oplus 0.6\text{mm}. \quad (5)$$

For the $K_{e2}/K_{\mu2}$ analyses, the starting samples are "one-track" triggers obtained by requiring hits in both views of the hodoscope. While in 2003 a downscaled unbiased sample of one-track events was obtained with a 12-hour run, in 2004 a 56-hour special run has been made with different triggers for K_{e2} and $K_{\mu2}$, the condition of having more than 10 GeV deposited in the LKr calorimeter being added for the first channel.

Data reduction for both samples is made by requiring only one track reconstructed by DCHS passing acceptance and quality cuts; the track must intercept the beam line with a small impact parameter in a point well within the decay volume, between 2 m and 8.5 m from the last collimator; the track momentum is required to be in the expected range for K_{l2} decays, $15 < p < 50$ GeV. These cuts reject much of the background from non-kaon events or early kaon decays. Background rejection for K_{e2} identification is performed by associating the track from DCHS with a LKr cluster: the ratio E/P of cluster energy and track momentum plotted for 2003 and 2004 data versus the missing mass (evaluated from track momentum) shows a clear peak corresponding to K_{e2} decays, see Fig. 5.

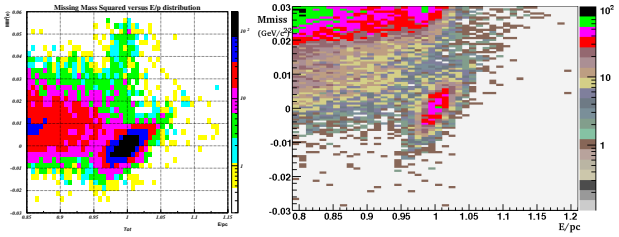

FIG. 5: Distributions of the missing mass squared of the secondary track in the electron mass hypothesis versus the ratio E/P of cluster energy in the LKr and track momentum. Left (right) panel refers to 2003 (2004) data.

The main background under the K_{e2} peak is due to $K_{\mu2}$ events in which the muon produces a "catastrophic" energy release in the LKr, with $E/P \sim 1$. A cut on $M_{\rm miss}$ is enough for clean identification of K_{e2} for low momentum tracks, namely $p <\sim 30$ GeV, while kinematics cannot be used at high momenta; see left panel of Fig. 6.

For the purpose of background subtraction in this range, the probability for a muon to produce a cluster with $E/P > 0.95$ has been evaluated from a selected muon sample and is $\sim 0.5 \times 10^{-6}$. The statistics of the sample used induces a significant error to the final result: for the preliminary result from 2004 data, the fractional statistical error due to K_{e2} counts is

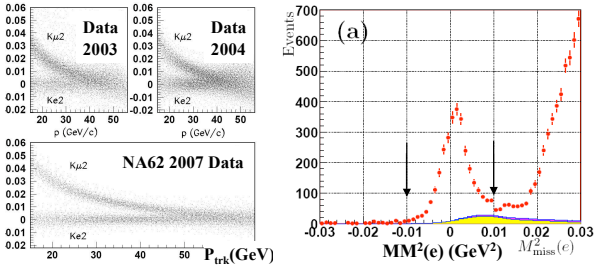

FIG. 6: Left: missing mass squared $MM^2(e)$ (GeV^2 units), evaluated in the electron mass hypothesis, as a function of the track momentum; different years of data taking are separately shown. Right: K_{e2} peak in the $MM^2(e)$ distribution for the 2007 NA62 run; a background estimate is also shown (filled histogram).

1.85%, while the systematic error due to background subtraction is 1.59%.

For these reasons, the experimental setup has been optimized by the NA62 Collaboration for the purpose of a new dedicated data taking during 2007: the average kaon momentum selected has been raised up to 75 GeV, the momentum bite has been lowered to 2.5%, and the transverse momentum kick induced by the analyzing magnet of the DCHS system has been increased by more than a factor of 2, up to 263 MeV. These features improve the $M_{\rm miss}$ resolution and maximize the kinematical separation of K_{e2} and $K_{\mu 2}$, see right panel of Fig. 6. For the evaluation of the probability for a muon to fake an electron in the LKr calorimeter, for part of the run a lead wall has been put in between the two hodoscope scintillator layers: this allows a direct measurement of the "catastrophic" energy loss probability from data. The data taking lasted for 4 months, and allowed the NA62 Collaboration to acquire the largest K_{e2} sample in the world, amounting to more than 10^5 events; see right panel of Fig. 6. The analysis is expected to measure R_K with a $< 0.5\%$ total error, thus improving significantly the sensitivity to new physics contributions (Fig. 7).

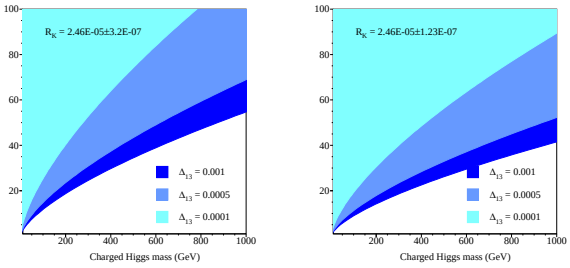

FIG. 7: Exclusion plots at 95% CL in the tan β-M_H plane from the present world average (left) or from a result with the same central value but a 0.5% error (right). Different values of the Δ_{13} LFV parameter of Ref. [24] are used.

[1] L. G. Landsberg, Phys. Atom. Nucl. **68**, 1190 (2005) [arXiv:hep-ph/0410261].
[2] E. Abouzaid *et al.* [KTeV Collaboration], Phys. Rev. Lett. **100**, 131803 (2008).
[3] A. Sirlin, *Rev. Mod. Phys.* **50**, 573 (1978); *Nucl. Phys. B* **196**, 83 (1982).
[4] V. Cirigliano *et al. Eur. Phys. J. C* **23**, 121 (2002).
[5] KLOE Coll., *Phys. Lett. B* **632**, 43 (2006).
[6] KLOE Coll., *Phys. Lett. B* **636**, 166 (2006).
[7] KLOE Coll., *Phys. Lett. B* **626**, 15 (2005).
[8] KTeV Coll., *Phys. Rev. D* **70**, 092006 (2004).
[9] NA48 Coll., *Phys. Lett. B* **602**, 41 (2004).
[10] NA48 Coll., *Phys. Lett. B* **602**, 41 (2004). L. Litov [NA48 Collaboration], arXiv:hep-ex/0501048.
[11] KLOE Coll., *JHEP* **0801**, 073 (2008).
[12] KLOE Coll., *JHEP* **0802**, 098 (2008).
[13] NA48/2 Coll., *Eur. Phys. J. C* **50**, 329 (2007).
[14] V. I. Romanovsky *et al.*, arXiv:0704.2052.
[15] KLOE Coll., *Phys. Lett. B* **636**, 173 (2006).
[16] KLOE Coll., *Eur. Phys. J. C* **48**, 767 (2006).
[17] FlaviaNet Working Group on Kaon Decays, arXiv:0801.1817 [hep-ph].
[18] Particle Data Group, *Phys. Lett. B* **592**, 1 (2004).
[19] Particle Data Group, *Phys. Lett. B* **667**, 1 (2008).
[20] W. S. Hou, *Phys. Rev. D* **48**, 2342 (1992).
[21] G. Isidori and P. Paradisi, *Phys. Lett. B* **639**, 499 (2006).
[22] G. Isidori and A. Retico, *JHEP* **11**, 001 (2001).
[23] Belle Coll., *Phys. Rev. Lett.* **97**, 251802 (2006). Babar Coll., arXiv:0705.1820 (2007).
[24] A. Masiero, P. Paradisi, and R. Petronzio, *Phys. Rev. D* **74**, 011701 (2006).
[25] V. Cirigliano and I. Rosell, arXiv:0707.4464 (2007).
[26] A. Sibidanov, arXiv:0707.4623 (2007).
[27] L. Fiorini, *Nucl. Phys. Proc. Suppl.* **169**, 205 (2007); V. Kozhuharov, *PoS* **KAON**, 049 (2007).
[28] KLOE Coll., *Nucl. Instrum. Methods A* **488**, 51 (2002).
[29] KLOE Coll., *Nucl. Instrum. Methods A* **482**, 364 (2002).
[30] NA48 Coll., Nucl. Instrum. Meth. A **574**, 433 (2007).